http://dx.doi.org/10.5935/0103-5053.20140273

J. Braz. Chem. Soc., Vol. 25, No. 12, 2455-2465, 2014.
Printed in Brazil - ©2014 Sociedade Brasileira de Química
0103 - 5053 $6.00+0.00

Article

Ni/La_2O_3-SiO_2 Catalysts Applied to Glycerol Steam Reforming Reaction: Effect of the Preparation Method and Reaction Temperature

Vivian V. Thyssen and Elisabete M. Assaf*

Instituto de Química de São Carlos, Universidade de São Paulo;
Av. Trabalhador Sãocarlense, 400, 13560-970 São Carlos-SP, Brazil

Catalisadores Ni/La_2O_3-SiO_2 foram preparados por diferentes métodos: impregnação sequencial, impregnação simultânea (I-sim), precipitação do suporte seguida da impregnação do metal e co-precipitação. As amostras foram caracterizadas por espectroscopia de energia dispersiva de raios X, fisissorção de nitrogênio, difração de raios X (XRD), espectroscopia de infravermelho, redução a temperatura programada (TPR), quimissorção de H_2, microscopia eletrônica de varredura e análise termogravimétrica. As análises de XRD e TPR indicaram duas espécies de Ni nas amostras: NiO (I-sim) e La_2NiO_4 (outras amostras). Foram realizados testes catalíticos na reação de reforma a vapor de glicerol a 600 °C. O melhor resultado foi observado com o catalisador I-sim, que apresentou o maior grau de redução, maior dispersão metálica e maior área metálica (TPR e TPD). Foram realizados testes a 500 e 700 °C com esse catalisador, que apresentou melhores resultados a 600 °C.

Ni/La_2O_3-SiO_2 catalysts were obtained by different methods of preparation: sequential impregnation, simultaneous impregnation (I-sim), precipitation of support followed by Ni impregnation and co-precipitation. The samples were characterized by energy-dispersive X-ray spectroscopy, nitrogen physisorption, X-ray diffraction (XRD), infrared spectroscopy, temperature programmed reduction (TPR), H_2 chemisorption, scanning electron microscopy and thermogravimetric analysis. XRD and TPR results indicated two Ni species in the samples: NiO (I-sim) and La_2NiO_4 (other samples). Catalytic tests were performed in glycerol steam reforming at 600 °C. The best result was observed with I-sim catalyst, which presented the higher reduction degree, metallic dispersion and metallic area (TPR and TPD). This catalyst was also tested at 500 °C and 700 °C and performed best at 600 °C.

Keywords: nickel, catalysts, preparation method, steam reforming, glycerol

Introduction

Biodiesel is a fuel derived from vegetable oils or animal fats. It is used in diesel engines, mixed in any proportion with mineral diesel.[1] As a fuel, biodiesel has some advantages over to petroleum fuels; for instance, it is virtually free of sulfur and aromatic compounds, and is nontoxic and biodegradable, as well as being derived from renewable sources.[2] The main synthetic route for biodiesel is the transesterification (equation 1) of vegetable oils with alcohols (methanol and ethanol), using basic catalysis.

$$\underset{\text{Glyceride}}{C_3H_5(OCOR_n)_3} + \underset{\text{Alcohol}}{3R'OH} \leftrightarrows \underset{\text{Ester}}{3R_nCOOR'} + \underset{\text{Glycerol}}{C_3H_5(OH)_3} \quad (1)$$

Under the action of a basic catalyst and in the presence of methanol or ethanol, the oil undergoes a transesterification to form three molecules of methyl or ethyl esters of fatty acids, which are essentially the biodiesel, and releases a molecule of glycerol as a byproduct.

For each 90 m^3 of biodiesel produced by transesterification, approximately 10 m^3 of glycerol is generated. Thus, the commercial viability of biodiesel depends on the consumption of this volume of glycerol, and large-scale applications are sought to add value to the productive chain.[3]

Currently, glycerol has a range of medium-scale industrial applications, especially in the manufacture of synthetic resins, ester gums, drugs, cosmetics and toothpaste.[1,4,5] A new and promising possible application for glycerol is in the production of hydrogen (H_2) for fuel cells.[6,7]

*e-mail: eassaf@iqsc.usp.br

Major processes used for H_2 production include the steam reforming of hydrocarbons, such as methane (CH_4) and naphtha, and alcohols. Methanol and ethanol have been extensively studied and now glycerol appears to be an attractive raw material for the process of steam reforming, owing to its low toxicity and high production of H_2 (equation 2).

$$C_3H_5(OH)_3 + 3H_2O \leftrightarrows 3CO_2 + 7H_2$$
$$\Delta H_r^o = 123.0 \text{ kJ mol}^{-1} \quad (2)$$

The important properties of steam-reforming catalysts (activity, selectivity, stability, strength, etc.) depend strongly on to their composition and preparation technique.

The general scheme for the preparation of supported catalysts includes the following steps: preparing the support or acquiring a commercial support, active species impregnation, drying, calcination and activation (this last step conducted *in situ*, immediately prior to the catalytic run).

Ni catalysts supported on various matrices show activity and selectivity suitable for the production of H_2 by steam reforming of alcohols, and it is suggested that Ni catalysts favor the breaking of the C–C bond of alcohols to form CH_4, H_2 and CO.[8-10]

Commercial SiO_2 is widely used as a support, owing to its high surface area. La_2O_3 has the capacity to prevent sintering of the Ni metallic phase and the deposition of carbon on its surface, thus minimizing the potential deactivation of the catalyst.[10]

Therefore, the objective of this study was to investigate the influence of the preparation method of Ni/La_2O_3-SiO_2 catalyst on the steam reforming of glycerol (SRG) for the production of H_2 at different temperatures.

Experimental

Preparation

Catalysts were prepared by four different methods, in which 10 wt.% Ni was deposited on a support composed of 30 wt.% La_2O_3-70 wt.% SiO_2 (30LaSi), which was chosen on the basis of a previous work.[10]

In the earlier study,[10] the catalysts were prepared by the sequential impregnation method. A commercial SiO_2 support (Degussa - Aerosil 200) was heated at 600 °C for 2 h under a flow of synthetic air, for thermal stabilization. The mixed supports (10 wt.% La_2O_3-90 wt.% SiO_2, 30 wt.% La_2O_3-70 wt.% SiO_2 and 50 wt.% La_2O_3-50 wt.% SiO_2) were prepared by impregnation of the treated SiO_2 with an aqueous solution of $La(NO_3)_3.6H_2O$ (Vetec), so as to give mass contents of 10, 30 and 50% La_2O_3 on SiO_2. Excess water was removed by rotary evaporation at 80 °C for 6 h and the samples were then dried at 80 °C for 12 h and calcined at 600 °C for 2 h, under a flow of synthetic air. The supports were then impregnated with an aqueous solution of $Ni(NO_3)_2.6H_2O$ (Aldrich) and the resulting precursors were dried and calcined for 3 h at 600 °C, under flowing synthetic air, to give catalysts with 10 wt.% Ni. Experimental tests showed that the best catalyst for the glycerol steam reaction was that supported on 30 wt.% La_2O_3-70 wt.% SiO_2. This sample was thus chosen for further study, being identified as 10Ni30LaSi (I-seq).

In the present study, the catalyst 10Ni30LaSi was also prepared by three other methods, to assess the effect of the preparation method on the catalytic performance.

Following I-seq, the second catalyst was prepared by the simultaneous impregnation method. In this case, the pretreated SiO_2 was impregnated with solutions of $La(NO_3)_3.6H_2O$ and $Ni(NO_3)_2.6H_2O$ simultaneously, dried and calcined as described above. This catalyst was named 10Ni30LaSi (I-sim).

The next catalyst was prepared by support precipitation, followed by metal impregnation, and the last one by the coprecipitation method. For the precipitation of the support, an aqueous suspension of SiO_2 was prepared and maintained by stirring. Na_2CO_3 (Synth) and $La(NO_3)_3.6H_2O$ solutions were added dropwise and the pH was adjusted to between 9 and 10 with 1 mol L^{-1} NaOH solution (Synth). The precipitate was then left to stand for a 12 h aging period, after which it was filtered and washed with distilled water until the residual NaOH was no longer detected. After washing, the samples were dried and finally subjected to a heating ramp (10 °C min^{-1}) at normal pressure under flow synthetic air until reaching 600 °C, where they were maintained for a period of 2 h. After the support was prepared, it was impregnated with Ni, following the steps described above, to yield the catalyst 10Ni30LaSi (P + I). For the catalyst prepared by coprecipitation, an aqueous suspension of SiO_2 was prepared and maintained by stirring, while the solutions of $La(NO_3)_3.6H_2O$, $Ni(NO_3)_2.6H_2O$ and Na_2CO_3 were added dropwise to achieve simultaneous precipitation. This catalyst was named 10Ni30LaSi (P).

Characterization

The samples were analyzed by energy-dispersive X-ray (EDX) spectroscopy, to determine their chemical composition, with a LEO 440 electron microscope (Leica Zeiss) coupled to an energy-dispersive analyzer of Si

(Li) with a beryllium window (Oxford 7060) and 133 eV resolution. For this analysis, the catalysts were formed into pellets, on which five different spots were analyzed, to calculate the mean composition of the sample.

The specific surface area of the samples was determined by N_2 physisorption (BET method), with a Quantachrome Nova 1000e instrument. The sample was treated under vacuum at 190 °C for 2 h for degassing. Then, it was transferred to the adsorption unit, where liquid nitrogen comes into contact with the sample and the analysis begins with the passage of adsorbate gas N_2. The pressures were varied and the adsorption phenomenon occurred.

The samples were characterized by powder X-ray diffraction (XRD), to identify the crystalline phases present, on a Rigaku Multiflex diffractometer with Cu Kα radiation. The Bragg angle (2θ) was scanned at 2 degree min^{-1}, between 10 degree and 80 degrees.

Fourier transform infrared spectroscopy (FTIR) spectra of fresh catalysts were recorded in a Bomem/MB-102 FTIR spectrometer. Self-supporting sample discs were pressed from KBr and catalysts.

Temperature-programmed reduction (TPR) was carried out in an Analytical Multipurpose System. The catalysts were reduced in a fixed-bed quartz reactor in an atmosphere of 1.96% H_2/Ar flowing at 30 mL min^{-1}, programmed with a 10 °C min^{-1} heating ramp from 25 °C to 1000 °C. The area under reduction peak is proportional to the total quantity of H_2 consumed in reduction process. By using standard data of CuO reduction, it was possible to calculate H_2 consumption for reduced species and the samples reducibility.

Metallic surface area and dispersion were obtained by means of H_2 chemisorption in Micromeritics (ChemiSorb 2750) equipment. The samples, placed in a quartz U-shaped reactor, were reduced at 600 °C for I-seq and 700 °C for the others for 1 h under 25 mL min^{-1} of a mixture 10% H_2/Ar. The chemisorption was performed at 25 °C by pulses of a mixture of 10% H_2/Ar in a flow of 25 mL min^{-1} of Ar. The metallic area of Ni was estimated assuming the stoichiometry $H_{adsorbed}/Ni_{surface} = 1$ and that a density of active sites on the surface of 1.54×10^{19} atoms m^{-2}.[11]

Scanning electron microscopy (SEM) images of the used catalysts were taken with a LEO-440 scanning electron microscope equipped with an Oxford detector.

Thermogravimetric analysis (TGA) experiments were performed in a Mettler Toledo Instruments TGA analyzer (TGA/DSC1), in order to estimate the different carbon formed on the catalysts. Approximately 10 mg of spent catalyst was heated in a stream of air from room temperature to 800 °C, at a rate of 10 °C min^{-1}, and the weight change was measured.

Catalytic tests

Glycerol steam reforming tests were performed in a tubular quartz reactor fed with water:glycerol in a molar ratio of 3:1, with a solution flow rate of 2.5 mL h^{-1} produced by a high-precision pump. For each reaction, were used 150 mg of catalyst, sieved in the range of 60-100 mesh, and $W F^{-1} = 0.05\ g_{cat}\ h\ g_{solution\ fed}^{-1}$, to avoid diffusion effects. The tests were performed at 600 °C for 5 h at atmospheric pressure. The catalyst that performed best was also tested at 500 °C and 700 °C for 5 h. Following these tests, a stability test, for 10 h, was performed on this catalyst at the temperature that afforded the best results. Before starting the reaction, the catalysts were activated *in situ* for 1 h by H_2 flowing at 30 mL min^{-1}, at temperatures determined in the TPR tests for each sample (600 °C for I-sim and 700 °C for the others). After activation, the system was purged with a flow of N_2 while it reached the reaction temperature.

The effluent was analyzed by gas chromatography on a Shimadzu system with H_2 as carrier gas and a capillary column HP5 operating between 35 °C and 250 °C, with a FID detector. We used external standards, known concentrations solutions, to obtain a calibration curve for glycerol. Based on the analytical curve, the concentration of unreacted glycerol contained in the samples was determined in mol L^{-1}, multiplying this concentration by the volume of effluent collected determined the number of moles of unreacted glycerol ($n_{residual}$) and the global glycerol conversion ($\%X_T$) was calculated from equation 3.

$$\%X_T = [(n_{total} - n_{residual})\ (n_{total})^{-1}]\ 100 \quad (3)$$

where, n_{total} is the number of moles of glycerol fed.

The glycerol conversion to gaseous products ($\%X_G$) was calculated from equation 4.

$$\%X_G = [\text{C mol in gas products}/(3\ n_{total})] \times 100 \quad (4)$$

The glycerol conversion to liquids products ($\%X_L$) was calculated from equation 5.[11]

$$\%X_L = \%X_T - \%X_G \quad (5)$$

A gas chromatograph (Varian GC-3800) with two columns operating in parallel, each with a thermal conductivity detector, was used for in-line analysis of the gaseous products of the reaction. The columns used were packed with Porapak-N and Molecular Sieve 13X, operating between 40 °C and 80 °C, with carrier gases He and N_2, respectively, flowing at 10 mL min^{-1}. Analytical curves were produced for H_2, CO, CO_2, CH_4 and C_2H_4. The

H_2 yield was calculated from equation 6 and yield to CO, CH_4, CO_2 and C_2H_4 (R_i) from equation 7.

$$H_{2yield} = (H_2 \text{ mol produced}) (n_{total})^{-1} \quad (6)$$

$$R_i = (mol_i \text{ produced}) (n_{total})^{-1} \quad (7)$$

Qualitative analysis was performed on the accumulated liquid reaction products after the end of the reaction by a GCMS-QP20105 system (Shimadzu), equipped with a column of rtx-wax (30 m × 1 μm × 0.32 mm); the temperature of the column rose from 40 °C to 200 °C and the temperature of the injector was 280 °C.

The quantity of carbon formed on the catalyst during the reaction was determined by an EA1110 CHNS-O Elemental Analyzer, equipped with a Porapak-PQS column.

Results and Discussion

Characterization

Table 1 shows the results of chemical analysis of the supports (La) and catalysts (Ni) by EDX.

Table 1. Mean contents of La and Ni and specific areas of the catalysts and supports

Preparation method	Content / wt.%		Specific area / (m^2 g^{-1})	
	Support (La) 30LaSi	Catalyst (Ni) 10Ni30LaSi	Support 30LaSi	Catalyst 10Ni30LaSi
I-seq[a]	29.6 ± 2.5	9.7 ± 1.2	101	138
I-sim	33.5 ± 1.8	9.8 ± 0.7	–	121
P+I	31.3 ± 1.9	11.9 ± 0.9	95	109
P	32.6 ± 1.0	10.6 ± 0.2	–	98
SiO_2[a]	–	–	231	–

[a]Data based on Thyssen *et al.*[10]

The contents measured were close to nominal levels (10 wt.% Ni and 30 wt.% La), showing that the methods of preparation were adequate. Small differences in the values resulted from the handling of the precursors during preparation.

Table 1 also shows the specific surface areas of the samples.

It can be seen that, independent of the preparation method employed, the addition of La on SiO_2-support causes a significant decrease in the specific area. This can be explained by the possible agglomeration of the particles during the process of preparation of such supports.[10,12]

It was observed that the support prepared by precipitation had a surface area 20% larger than the support prepared by impregnation. This may be related to the fact that the precipitation occurred under conditions of supersaturation, where the precipitation rate was high, with the aim of forming small particles. Under these conditions, the nucleation rate is greater than the rate of crystal growth. Nucleation is the step where the molecules dissolved in the solvent begin to form clusters, on the nanometer scale. These clusters are the core of the future crystal and only become stable from a critical size, which depends on the operating conditions (temperature, supersaturation, irregularities, etc). If the cluster does not achieve stability, it dissolves again. The growth of a crystal on the core occurs when the cluster has reached the critical size. Nucleation and growth occur simultaneously, but a condition of supersaturation normally favors the formation of new clusters. These clusters are small particles with large specific surface areas. Most of the crystal growth occurs during aging, when the suspension is allowed to stand for a period - in the present case, this period may have been insufficient for large crystals to be generated, thus increasing the specific area of the precipitated material.

The growth of crystals in the aging period was possibly more efficient than in the case of the catalyst prepared by co-precipitation, since this had a lower specific area.

For I-seq and P + I catalysts an increase in the value of specific area with Ni impregnation was observed. In this case, Ni species present in the catalyst contributed to the increase in total area.[10,12]

Figure 1a displays the XRD patterns of the supports.

XRD patterns of the supports show that the preparation method influenced the crystalline structure of the material. The support prepared by impregnation produced a pattern with a plateau that can be divided between the species SiO_2 (JCPDS 83-2473) and La_2O_3 (JCPDS 83-1344) well dispersed (2θ ca. 23 degree and 30 degree), and another broad peak at 2θ ca. 45 degree, also attributed to La_2O_3. In the diffractogram of the support prepared by La_2O_3 precipitation in a suspension of SiO_2, there are peaks related to La_2O_3 and $La(OH)_3$ (JCPDS 36-1481) species, but the shoulder for SiO_2 species was hidden. The $La(OH)_3$ phase would be formed during the precipitation at high pH, by reaction of NaOH with $La(NO_3)_3$ to form $La(OH)_3$.[13]

For amorphous materials, which do not have regular crystal planes or long-range structure, broad and low or no peak are expected. This may be the case of the P + I support, indicating that the SiO_2 in this compound has low crystallinity.[10]

The XRD patterns of the catalysts prepared by sequential impregnation (I-seq), simultaneous impregnation (I-sim), Ni impregnation on a precipitated support (P + I) and co-precipitation (P) are shown in Figure 1b. The only

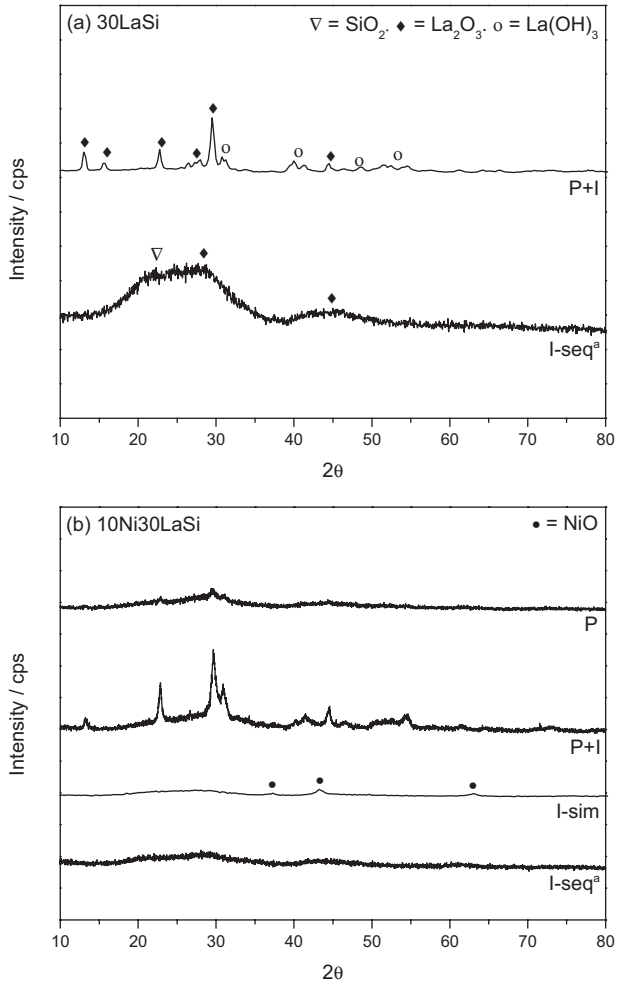

Figure 1. XRD patterns of (a) supports and (b) catalysts. [a]Data based on Thyssen *et al*.[10]

catalyst which showed peaks for the crystal structure of NiO (JCPDS 78-0643) was that prepared by simultaneous impregnation. This suggests that in the other catalysts, the Ni species were more finely dispersed on the support, occasionally forming $LaNiO_3$ and/or $LaNiO_4$ species that would display peaks coinciding with those of La_2O_3 and/or $La(OH)_3$ species.[13]

In temperature-programmed reduction, none of the supports showed any reduction in the temperature range examined. Thus, the peaks observed in catalyst TPR profiles (Figure 2) were assigned to various Ni species.

The peak at about 700 °C in the TPR profiles of the catalysts 10Ni30LaSi (I-seq), 10Ni30LaSi (P + I) and 10Ni30LaSi (P) belongs to the La_2NiO_4 surface species, which is reduced by H_2 above 600 °C.[12] These peaks refer to a kind of Ni oxide described as a bound state, because it exhibits relatively great interaction with the support and thus a higher reduction temperature than free NiO; this peak may thus be attributed to reduction of La_2NiO_4 on the surface of the material.[10] The peak at 900 °C in the profile of the catalyst 10Ni30LaSi (P + I) can be attributed to reduction of the La_2NiO_4 species in the bulk of the material.[14] La_2NiO_4 may be formed as amorphous species since showed no peaks in the XRD patterns of these catalysts (I-sim, P + I and P).[10,13]

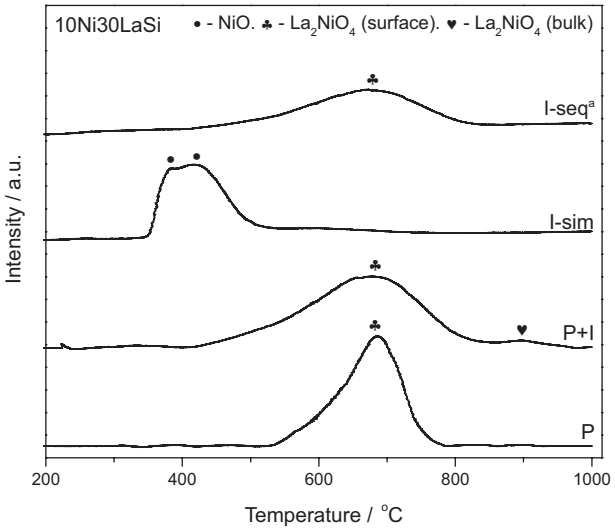

Figure 2. TPR profiles of catalysts. [a]Data based on Thyssen *et al*.[10]

The catalyst 10Ni30LaSi (I-sim) shows two peaks for NiO, indicating two different interactions with the support: the peak at 380 °C represents the reduction of NiO, which hardly reacts at all with the support, while the second peak (420 °C) refers to reduction of NiO interacting weakly with the support.[15] Because of its high mobility on the surface of the material, which leads to the easy migration and aggregation of particles, such NiO is easily reduced and is described as a free state of the Ni active phase.[16]

In the method of sequential impregnation (I-seq), the lanthanum oxide precursor is initially adsorbed on the commercial support, forming La_2O_3-SiO_2 at the interface; subsequently, NiO is adsorbed on the La_2O_3, forming La_2NiO_4. In contrast, in I-sim, both the lanthanum and nickel oxides compete for adsorption sites on the silica in the method of simultaneous impregnation. Therefore, the catalyst prepared by simultaneous impregnation is not expected to provide a very homogeneous surface and La_2NiO_4 is not formed, because the La_2O_3 is not uniformly dispersed over the silica before the Ni adsorption takes place.[17]

The TPR analysis results agree with the XRD patterns of these catalysts, since the only catalyst that showed peaks for the NiO crystal structure (I-sim, Figure 1b) was the only catalyst that showed reduction of this species.

As noted in Table 1, there was an increase in the surface area of the support with the impregnation of Ni for samples I-seq and P + I, this may occur due to the formation of

species that contributed to the material surface area, as already pointed. It was observed the presence of La_2NiO_4 for these two catalysts, thus its area (9.3 $m^2 g^{-1}$)[14] may have been added to the support area then resulting in an increase in the area of these catalysts.

Table 2 shows the activation temperature chosen for the catalysts from the TPR results, H_2 consumption during the reduction of NiO and La_2NiO_4, the degree of reduction of the catalytic metal, the metallic dispersion on catalyst surface and metallic area.

Even with the reduction peak at 800 °C, the chosen activation temperature of P + I catalyst was 700 °C, which occurred the highest H_2 consumption in its reduction. Thus, the possibility of sintering decreases considerably, since the sample was calcined and tested at 600 °C.

It can be seen that the catalyst 10Ni30LaSi (P) showed the lowest reducibility, metallic dispersion and metallic surface area, which would be deleterious to the process of glycerol steam reforming, since the active phase of the catalyst is Ni in metallic and not the oxidized state. Thus, low reducibility of the catalyst would lead to a smaller density of active sites, causing impairment of the reaction.

It may be noted that the catalysts present the same behavior regarding the reduction degree, metallic dispersion and metallic surface area, and showed the following order for these parameters: P < I-seq < P + I < I-sim.

It was expected that the catalysts that presented bound state Ni species on the surface to present a greater metallic dispersion, since it Ni interacts more strongly with the support in these cases.[10,12] However, even these catalysts presenting a good dispersion (with exception of P catalyst), the I-sim catalyst showed a better metallic dispersion, as well as a higher metallic surface area and a higher reduction degree of Ni species. The presence of free state Ni species in this catalyst might be the reason for these results, since NiO is apparently more accessible to reduce than the La_2NiO_4, in these cases.[11]

The catalysts were analysed by FTIR spectroscopy. The spectra are shown in Figure 3.

The absorption band at 3500 cm^{-1} arose from free or absorbed water in the sample, or possibly from $La(OH)_3$ species formed during the preparation of the precipitated

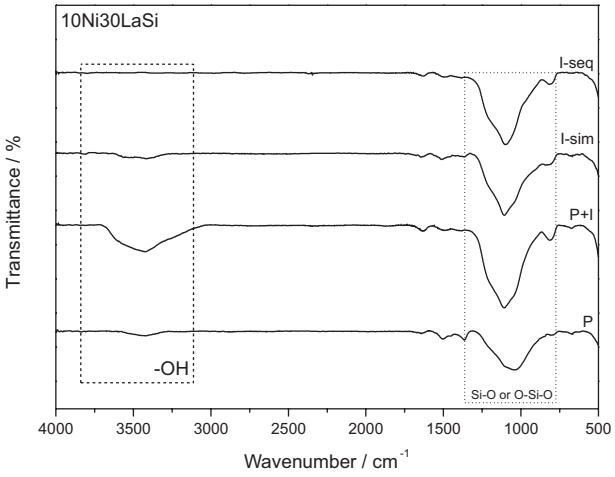

Figure 3. FTIR of catalysts.

catalysts, as shown in the XRD pattern of 10Ni30LaSi (P + I). This indicates the adsorption of water on samples during preparation.

The absorption bands between 800 and 1080 cm^{-1} can be attributed to various vibrations of Si–O or O–Si–O.[18] According to Zakaria *et al.*,[19] these bands may be associated with asymmetric stretching vibrations of the Si–O–Si group.

It was not possible to detect the metal in the catalyst since the peak for bare metal ions of Ni(II), at 930 cm^{-1}, could not be detected clearly in any of the spectra.[19]

Catalytic tests

Table 3 shows the results of glycerol steam reforming reaction.

A test without catalyst was also carried out to observe the performance of glycerol under reaction conditions used in this study (Table 3).

Glycerol, in the absence of catalyst, presents a high global conversion; however it shows only 10% of conversion to gaseous products, indicating that most of the glycerol was converted to liquid products. Only minimal amounts of H_2 and CO were observed among the gaseous products, which may be suggested that glycerol is thermally decomposed under the conditions studied (equation 8).

Table 2. Results of temperature programmed reduction and H_2 chemisorption

Preparation method	Activation temperature / °C	H_2 consumption (× 10^{-5}) / mol		Reduction[a] / %	D_M[b] / %	S_M[c] / ($m^2 g^{-1}$)
		NiO	La_2NiO_4			
I-seq	700	–	4.1	82	26	4
I-sim	600	9.6	–	100	40	14
P + I	700	–	5.0	86	32	6
P	700	–	2.6	48	14	2

[a]Degree of reduction of oxide phases; [b]metallic dispersion; and [c]metallic area.

$$C_3H_5(OH)_3 \rightarrow 3CO + 4H_2 \qquad \Delta H_r^o = 339.6 \text{ kJ mol}^{-1} \quad (8)$$

It may be noted that, for the reactions with catalysts, the volume of liquid collected from the effluent gas is inversely related to the global glycerol conversion achieved by the catalyst, lower conversion being reflected in the amount of unconverted glycerol in the effluent. This effluent liquid was analyzed qualitatively and the following compounds were identified, along with unreacted water and glycerol: propanoic acid, acetic acid, 2-propanone, formic acid, ethanol, propylene glycol, glycidol, 1,3-dioxane and sorbitol, as well as other, more complex, products.

Literature shows that the global conversion of glycerol with Ni catalysts is within the range of 60 to 100%, whereas its conversion into gaseous products is between 35 and 95%.[11,20,21] By comparing Table 3 and Table 2, it can be seen that the conversion of glycerol may be related to the degree of reduction, the metallic dispersion and metallic surface area of the catalytic material, since 10Ni30LaSi (P), which exhibited the lowest results for theses parameters, also showed the lowest glycerol conversion in the reaction. Moreover, the degrees of reduction, the metallic dispersions and metallic surface areas of the other catalysts followed the same order as the conversion of glycerol in their reactions: I-seq < P + I < I-sim.

The low selectivity for gaseous products on catalyst 10Ni30LaSi (P) shows that, besides the low conversion of glycerol and carbon produced, the catalyst did not favor the glycerol reforming reaction and did not show selectivity for the decomposition reactions of glycerol to gas and/or carbon. Since this catalyst resulted in a large volume of liquid effluent collected, it can be suggested that most of the reacted glycerol was converted into liquid products. Analyzing the gaseous product selectivity (Table 3 and Figure 4a), the catalyst 10Ni30LaSi (P) can be described as inactive for this reaction. The low reducibility, metallic dispersion and metallic area of this material (Table 2) may be responsible for the lack of catalytic activity, since the active phase of the catalyst is Ni in its reduced form and this catalyst was insufficiently reduced to exhibit activity in glycerol steam reforming.

The other three catalysts, prepared by the methods of the precipitation of the support followed by Ni impregnation: P + I (Figure 4b), sequential impregnation: I-seq (Figure 5a)

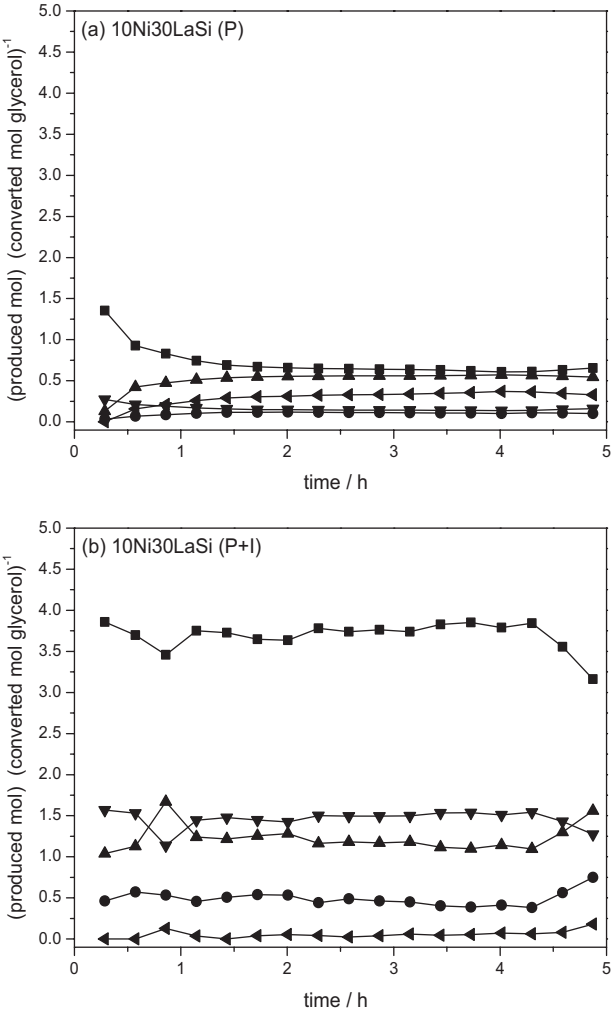

Figure 4. Gaseous products formed during the steam reforming of glycerol: (a) P, (b) P + I. (■ H_2; ● CH_4; ▲ CO; ▼ CO_2; ◀ C_2H_4).

Table 3. Results of steam reforming of glycerol

Catalyst 10Ni30LaSi	H_{2yield} / (mol mol^{-1})	CH_4[a] / (mol mol^{-1})	CO[a] / (mol mol^{-1})	CO_2[a] / (mol mol^{-1})	C_2H_4[a] / (mol mol^{-1})	H_2/CO_2 / (mol mol^{-1})	CO_2/CO / (mol mol^{-1})	C[b] / (produced mmol) (converted mol glycerol)$^{-1}$ h^{-1}	Liquid effluent[c] / mL	X_G[d] / %	X_L[e] / %	X_T[f] / %
I-seq[g]	2.8	0.2	0.7	1.1	t	2.8	1.6	1.1	5.8	67	12	79
I-sim	3.8	0.4	1.1	1.5	t	2.5	1.4	1.0	3.8	98	2	100
P + I	3.3	0.4	1.1	1.3	t	2.5	1.2	1.1	4.2	93	2	95
P	0.4	0.1	0.5	0.2	t	3.7	0.4	0.06	9.6	27	36	63
No catalyst	0.4	t	0.3	–	–	–	–	–	12.0	10	49	59

[a]C gaseous product yield; [b]carbon formation rate; [c]volume of liquid effluent collected; [d]glycerol conversion to gaseous products; [e]glycerol conversion to liquid products; [f]global glycerol conversion in 5-h reaction at 600 °C; [g]data based on Thyssen *et al.*;[10] t = traces < 0.1 (produced mol) (mol glycerol fed)$^{-1}$.

and simultaneous impregnation: I-sim (Figure 5b) proved to be active in the reaction.

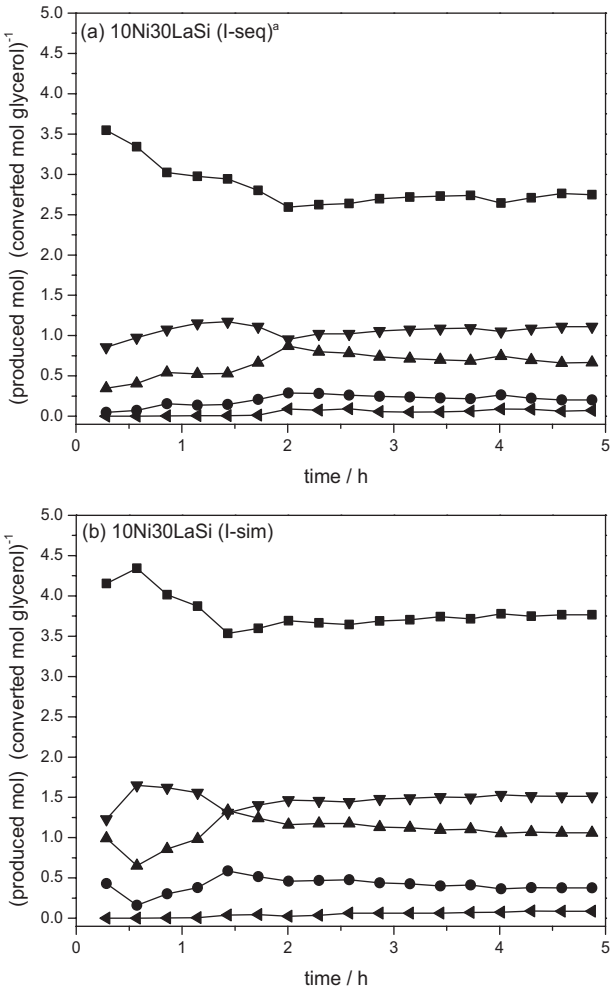

Figure 5. Gaseous products formed during the steam reforming of glycerol: (a) I-seq[a] and (b) I-sim. (■ H_2; ● CH_4; ▲ CO; ▼ CO_2; ◀ C_2H_4). [a]Data based on Thyssen *et al.*[10]

It can be seen that the H_2 and CO_2 yield, products expected for the reaction of steam reforming of glycerol (equation 2), followed the same order as the results presented on Table 2 for these three catalysts: I-seq < P + I < I-sim. Thus, it can be said that the higher reduction degree, metallic dispersion and metallic area of the catalyst, is expected a higher conversion of glycerol to the desired gaseous products in steam reforming of glycerol (equation 2), since the metallic Ni is the active phase for this reaction. Dieuzeide *et al.*[11] showed that H_2 and CO_2 yield increased linearly with Ni metallic area.

Probably, the reason for this result, is a greater availability of the Ni metallic present in the I-sim catalyst compared with the other catalysts wherein the Ni metallic stemmed to bound state species and might be less accessible on the surface to catalyze the reaction.

For the reaction of steam reforming of glycerol (equation 2), the theoretical H_2/CO_2 ratio would be about 2.3 (mol × mol^{-1}). It is seen in Table 3 that the experimental ratios were slightly higher, but close to stoichiometric.

The byproducts CO, CH_4 and C_2H_4 are produced by reactions that occur in parallel with the glycerol steam reforming reaction (equation 2) and these vary with the reaction conditions, such as temperature, pressure, catalyst type and water/alcohol ratio.[22] For example, CO can be produced by glycerol decomposition (equation 8).[23]

It has been shown that the amount of CO derived from the reforming reaction can be reduced by the water-gas shift reaction (equation 9). Hence, CO can be used to produce an additional amount of H_2.[22]

$$CO + H_2O \leftrightarrows CO_2 + H_2 \qquad \Delta H_r^o = -41.0 \text{ kJ mol}^{-1} \quad (9)$$

Thus, the CO_2/CO stoichiometric ratio would be 1, and Table 3 shows that, for those catalysts that were active in SRG, this ratio was higher than the theoretical value, showing that the catalysts had greater selectivity for CO_2 than for CO.

The catalysts 10Ni30LaSi (I-sim) and 10Ni30LaSi (P + I) exhibited better conversion of glycerol and greater selectivity for H_2 and CO_2 than 10Ni30LaSi (I-seq). Between these two catalysts, there was practically no difference in average selectivities of the gaseous products and formation of carbon. The catalyst 10Ni30LaSi (P + I) showed good H_2 selectivity and good conversion of glycerol (Table 3), but its H_2 and CO_2 selectivities decreased in the last hour of reaction, while the CO and CH_4 selectivities increased (Figure 4b). This behavior may suggest a partial deactivation of the catalyst during the reaction of steam reforming of glycerol.

I-sim showed a fall in H_2 production at the beginning of the process and was then stable throughout the reaction (Figure 5b), with the highest conversion of glycerol to gaseous products and the highest H_2 yield (Table 3). The first hour deactivation that this catalyst presents can be due to the stabilization time of the system, since this catalyst remained stable until the end of this process after the first hour.

Figure 6 presents the SEM images of P + I and I-sim catalysts after catalytic tests.

SEM images provide clear evidence of filamentous whiskers being deposited during the reaction to the I-sim catalyst.

The formation of carbon filaments was not observed on the surface of catalyst P + I as in the case of I-sim.

Figure 7 shows the weight loss profiles obtained by TG-DTG for I-sim and P + I spent catalysts.

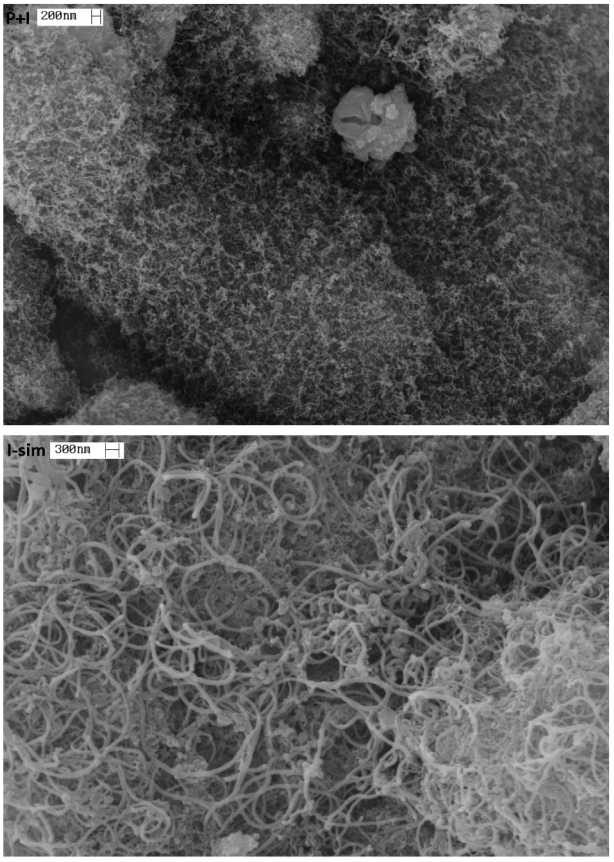

Figure 6. SEM images of P + I and I-sim after reaction.

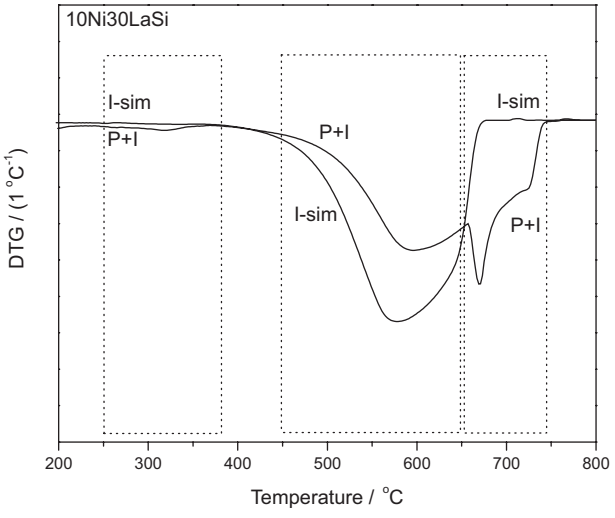

Figure 7. DTG: P + I and I-sim after reaction.

TG analyses of the I-sim and P + I used catalysts showed some differences concerning stability of the carbon deposits formed during glycerol steam reforming. Both catalysts show a broad peak related to weight loss due to carbon oxidation between 450 and 650 °C.

DTG profile of P + I catalyst presents also others regions of weight loss, suggesting differences in the nature of carbonaceous deposits. It is known that amorphous carbon presents peak of oxidation at low temperatures and filamentous carbon at high temperatures, while graphitic carbon needs higher temperature to be removed.[24-26] The P + I catalyst produced a small weight loss peak at around 320 °C, which is ascribed to amorphous carbon.[24]

The broad peak between 450 and 650 °C, for both catalysts, may be attributed to the combustion of graphitic carbon (graphitic filamentous carbon or polymorphic forms of graphite).[25,26] This peak to I-sim catalyst showed a superior carbon weight loss, revealing a much larger of graphitic carbon accumulation, as evidenced in the SEM images (Figure 6).

The P + I catalyst also produced a weight loss peak at around 700 °C, suggesting the presence of stable carbon deposits.[24] The presence of this nature of carbon deposits on P + I catalyst might be the reason to the deactivation of this catalyst at the last hour of reaction (Figure 4b).

The amount of carbon deposited during the reactions was very similar for both catalysts, showing that the Ni species present in the samples influence the type of carbon formed, but not of its quantity.

Table 4 shows the reaction results for 5 h on stream, with the catalyst 10Ni30LaSi (I-sim), at three different temperatures, and for a 10-h stability test at 600 °C.

With increasing temperature, the global conversion of glycerol tended to increase, and the volume of effluent collected at the end of the reaction decreased. However, the glycerol conversion to gaseous products was 98% at 600 °C, while at 500 °C and 700 °C was 30% and 73%, respectively. Thus, even at 700 °C, the catalyst showed a complete conversion of glycerol, some of it was converted into liquid products.

It can be seen in Table 3 and 4 that the catalysts showed H_2/CO_2 ratios very close to the theoretical value (2.3) or higher, at all tested temperatures, so that the H_2 selectivity is greater than the CO_2 selectivity at all temperatures.

The CO_2/CO ratio falls with rising temperature, showing that the exothermic shift reaction (equation 4) is favored at lower temperatures. The CO selectivity increases with increasing temperature of reaction, while the H_2, CH_4 and CO_2 selectivities were maximum at 600 °C.

The temperature variation may influence the formation of carbon during steam reforming reactions. It can be seen that increasing the temperature causes a decrease in the carbon deposition.

Carbon may be formed by CO decomposition, leading to the formation of CO_2 and C by the Boudouard reaction (equation 10).

$$2CO \leftrightarrows CO_2 + C \qquad \Delta H_r^o = -172.6 \text{ kJ mol}^{-1} \qquad (10)$$

Table 4. Results of steam reforming of glycerol at different temperatures and stability reaction

10Ni30LaSi (I-sim)	H_{2yield} / (mol mol^{-1})	CH_4[a] / (mol mol^{-1})	CO[a] / (mol mol^{-1})	CO_2[a] / (mol mol^{-1})	C_2H_4[a] / (mol mol^{-1})	H_2/CO_2 / (mol mol^{-1})	CO_2/CO / (mol mol^{-1})	C[b] / (produced mmol) (converted mol glycerol)$^{-1}$ h^{-1}	Liquid effluent[c] / mL	X_G[d] / %	X_L[e] / %	X_T[f] / %
500 °C (5 h)	1.3	0.3	0.1	0.5	–	2.4	7	1.2	4.3	30	47	77
600 °C (5 h)	3.8	0.4	1.1	1.5	t	2.5	1.4	1.0	3.8	98	2	100
700 °C (5 h)	3.1	0.1	1.3	0.8	–	3.9	0.6	0.7	2.8	73	27	100
600 °C (10 h)	4.1	0.4	1.2	1.3	t	3.2	1.1	0.9	6.6	97	3	100

[a]C gaseous product yield; [b]carbon formation rate; [c]volume of liquid effluent collected; [d]glycerol conversion to gaseous products; [e]glycerol conversion to liquid products; [f]global glycerol conversion, for I-sim; t = traces < 0.1 (produced mol) (mol glycerol fed)$^{-1}$.

The occurrence of the Boudouard reaction on Ni catalysts should be considered, since the presence of nickel in the form of the crystallites (NiO) observed for the catalyst I-sim (TPR and XRD) favors the diffusion of C atoms through the Ni. This diffusion process occurs more easily in these Ni crystallites because this oxide species does not interact so strongly with the support, so the carbon atoms are more easily introduced at the surface between the metal and the support.[27]

Since the Boudouard reaction (equation 10) is an exothermic reaction, like the water-gas shift reaction (equation 9), it is favored at lower temperatures. Therefore, the formation of carbon by the disproportionation of CO is not favored at 700 °C, this fact may also explain the higher CO selectivity at this temperature.

The formation of carbon at 700 °C may be due to the dissociation of CH_4 (equation 11), which is an endothermic reaction, favored at high temperatures. CH_4 dissociation would also explain the low selectivity observed at 700 °C for this product, as it would be consumed in the formation of C.

$$CH_4 \leftrightarrows 2H_2 + C \qquad \Delta H_r^o = 74.9 \text{ kJ mol}^{-1} \quad (11)$$

The low selectivity of methane could also be related to the methane steam reforming reaction (equation 12), as this would also be favored at high temperatures.

$$CH_4 + H_2O \leftrightarrows 3H_2 + CO \qquad \Delta H_r^o = 205.4 \text{ kJ mol}^{-1} \quad (12)$$

As can be seen in Figure 8, the catalyst 10Ni30LaSi (I-sim) was stable during the SRG reaction, at both 500 °C and 700 °C.

The stability test with the 10Ni30LaSi (I-sim) catalyst (Table 4 and Figure 9) showed that the catalyst was stable and yielded results close to those in the catalytic test performed for 5 h at 600 °C.

Conclusions

It is concluded that the method of preparation influences the physicochemical properties of the material, such as its specific surface area and the Ni species formed during the preparation. I-sim catalyst, that only presented NiO in its surface, showed the higher reduction degree, metallic dispersion and metallic area. This fact leads us to the conclusion that the free state of Ni is more accessible to reduce on the activation process.

In the catalytic tests, the catalysts I-sim and P + I exhibited similar H_2 selectivity, conversion of glycerol and

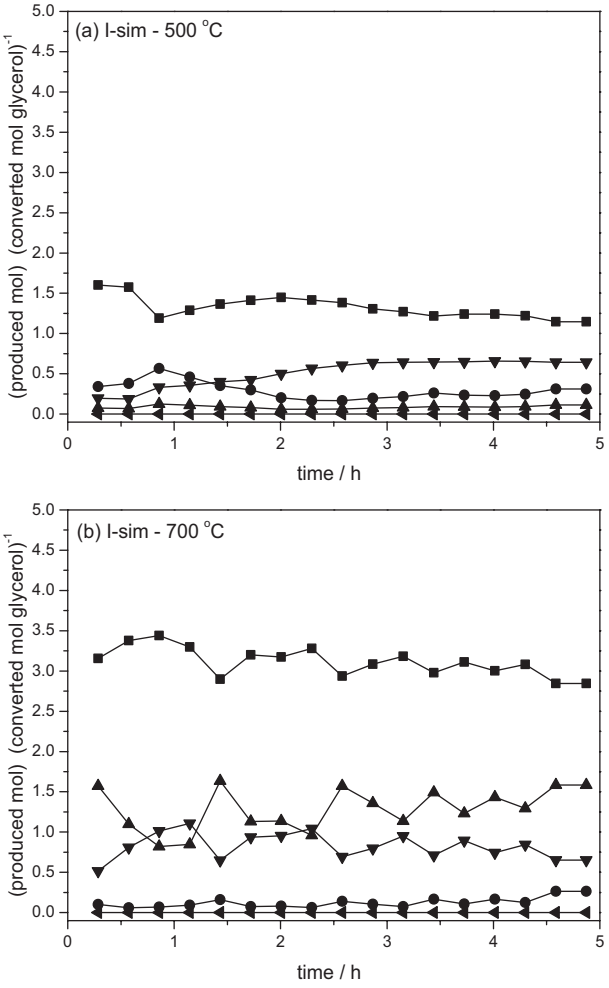

Figure 8. Gaseous products formed during the steam reforming of glycerol, on 10Ni30LaSi (I-sim): (a) 500 °C and (b) 700 °C. (■ H_2; ● CH_4; ▲ CO; ▼ CO_2; ◀ C_2H_4).

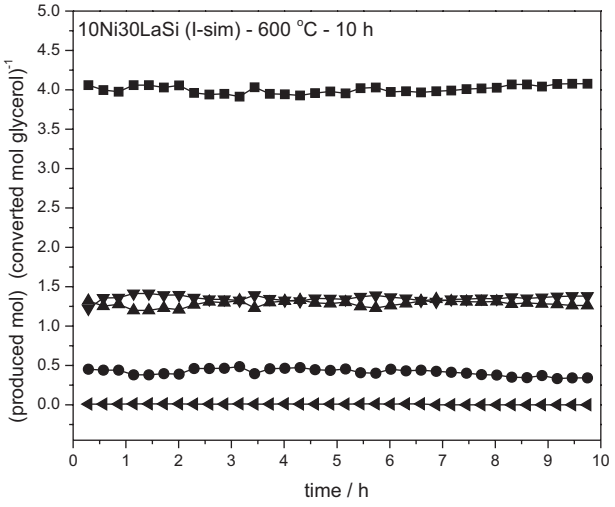

Figure 9. Gaseous products formed during the reaction of steam reforming of glycerol on 10Ni30LaSi (I-sim) over 10 h at 600 °C. (■ H_2; ● CH_4; ▲ CO; ▼ CO_2; ◀ C_2H_4).

carbon formation. However, the catalyst P + I showed a drop in H_2 selectivity towards the end of 5 h of reaction. This deactivation process of P + I catalyst may be explained by the presence of stable carbon deposited along the reaction, since that the I-sim catalyst showed a higher deposition of filamentous carbon, which is easier oxidized along the reaction.

With reactions at different temperatures using the I-sim catalyst, it is further concluded that the temperature is an important factor for steam reforming of glycerol. It may be noted that, according to the temperature, reactions that occur in parallel with the steam reforming of glycerol are favored or inhibited.

The I-sim catalyst performed best at 600 °C, and remained stable during the reaction for 10 h.

Acknowledgements

The authors thank CNPq, CAPES, USP/NAP-CiTecBio and FAPESP for financial support and the Electrochemistry Group at IQSC (USP, São Carlos, Brazil) for XRD analyses.

References

1. http://www.biodieselbr.com/biodiesel.htm accessed on August 14, 2013.
2. Barbosa, R. L.; da Silva, F. M.; Salvador, N.; Volpato, C. E. S.; *Ciênc. Agrotec.* **2008**, *32*, 1588.
3. Mota, C. J. A.; Da Silva, C. X. A.; Gonçalves, V. L. C.; *Quim. Nova* **2009**, *32*, 639.
4. http://anp.gov.br/?id=474 accessed on August 14, 2013.
5. Arruda, P. V.; Rodrigues, R. C. L. B.; Felipe, M. G. A.; *Revista Analytica* **2007**, *26*, 56.
6. Sun, J.; Qiu, X.; Wu, F.; Zhu, W.; Wang, W.; Hao, S.; *Int. J. Hydrogen Energy* **2004**, *29*, 1075.
7. Fierro, V.; Akdim, O.; Provendier, H.; Mirodatos, C.; *J. Power Sources* **2005**, *145*, 659.
8. Maia, T. A.; Bellido, J. D. A.; Assaf, E. M.; Assaf, J. M.; *Quim. Nova* **2007**, *30*, 339.
9. Mariño, F.; Baronetti, G.; Jobbagy, M.; Laborde, M.; *Appl. Catal., A* **2003**, *238*, 41.
10. Thyssen, V. V.; Maia, T. A.; Assaf, E. M.; *Fuel* **2013**, *105*, 358.
11. Dieuzeide, M. L.; Jobbagy, M.; Amadeo, N.; *Catal. Today* **2013**, *213*, 50.
12. Chica, A.; Sayas, S.; *Catal. Today* **2009**, *146*, 37.
13. Gao, J.; Hou, Z.; Guo, J.; Zhu, Y.; Zheng, X.; *Catal. Today* **2003**, *131*, 278.
14. Liu, B. S.; Au, C. T.; *Catal. Lett.* **2003**, *85*, 165.
15. Kirumakki, S. R.; Shpeizer, B. G.; Sagar, G. V.; Chary, K. V. R.; Clearfield, A.; *J. Catal.* **2006**, *242*, 319.
16. Xu, Z.; Li, Y.; Zhang, J.; Chang, L.; Zhou, R.; Duan, Z.; *Appl. Catal., A* **2001**, *210*, 45.
17. Therdthianwong, S.; Siangchin, C.; Therdthianwong, A.; *Fuel Process. Technol.* **2008**, *89*, 160.
18. Wu, C.; Williams, P. T.; *Appl. Catal., B* **2011**, *102*, 251.
19. Zakariaa, Z. Y.; Linnekoskib, J.; Amin, N. A. S.; *Chem. Eng. J.* **2012**, *207-208*, 803.
20. Nichele, V.; Signoretto, M.; Menegazzo, F.; Gallo, A.; Dal Santo, V.; Cruciani, G.; Cerrato, G.; *Appl. Catal., B* **2012**, *111-112*, 225.
21. Buffoni, I. N.; Pompeo, F.; Santori, G. F.; Nichio, N. N.; *Catal. Commun.* **2009**, *10*, 1656.
22. Farrauto, R.; Hwang, S.; Shore, L.; Ruettinger, W.; Lampert, J.; Giroux, T.; Liu, Y.; Ilimich, O.; *Annu. Rev. Mater. Res.* **2003**, *33*, 1.
23. Avasthi, K.; Reddy, R.; Patel, S.; *Procedia Eng*. **2013**, *51*, 423.
24. Carrero, A.; Calles, J. A.; Vizcaíno, A. J.; *Chem. Eng. J.* **2010**, *163*, 395.
25. Barroso, M. N.; Galetti, E.; Gomez, M. F.; Arrúa, L. A.; Abello, M. C.; *Chem. Eng. J.* **2013**, *222*, 142.
26. Maia, T. A.; Assaf, J. M.; Assaf, E. M.; *Fuel Process. Technol.* **2014**, *128*, 134.
27. Bradford, M. C. J.; Vannice, M. A.; *Appl. Catal., A* **1996**, *142*, 73.

Submitted on: August 6, 2014
Published online: November 21, 2014

FAPESP has sponsored the publication of this article.